Green and blue materials for the ceramic industry from pink MgCo$_x$Ni$_{1-x}$SiO$_4$ (0 ≤ x ≤ 1) solid solutions

M.A. Tena [a,*], Rafael Mendoza [b], Camino Trobajo [c], José R. García [c], Santiago García-Granda [d]

[a] *Inorganic Chemistry Area, Inorganic and Organic Chemistry Department, Jaume I University, P.O. Box 224, Castellón, Spain*
[b] *Physical Chemistry Area, Scientific and Technical Services, Oviedo University, CINN, Spain*
[c] *Inorganic Chemistry Area, Organic and Inorganic Chemistry Department, Oviedo University, CINN, Spain*
[d] *Physical Chemistry Area, Physical and Analytical Chemistry Department, Oviedo University, CINN, Spain*

ABSTRACT

In this study, MgCo$_x$Ni$_{1-x}$SiO$_4$ (0.0 ≤ x ≤ 1.0) solid solutions with an olivine structure were synthetized via the chemical coprecipitation method and materials with a smaller M(II) (M = Co, Ni) amount than Co$_2$SiO$_4$ and Ni$_2$SiO$_4$ compounds were obtained. At 1200 °C, the Co(II) and Ni(II) were randomly distributed in the MgCo$_x$Ni$_{1-x}$SiO$_4$ (0.0 ≤ x ≤ 1.0) solid solutions with the olivine structure, but the occupation of Co(II) and Ni(II) ions in M1 (4a) octahedral sites was obtained at a higher level than in M2 (4c) octahedral sites. The Mg(II) ions prefer the M2 sites. This preference explains the main contribution of the M1 sites in spectra of octahedral Co(II) ions and the M1-O and M2-O distances jointly explain the pink colour of the MgCo$_x$Ni$_{1-x}$SiO$_4$ (0.0 ≤ x ≤ 1.0) solid solutions, while the colour of Co$_2$SiO$_4$ is blue. Spectra can be interpreted as the sum of Ni(II) and Co(II) ions in octahedral sites. When these solid solutions are enamelled, the pink colouring changes to green or blue because of the presence of tetrahedral Co(II).

1. Introduction

Yellow-green Ni$_2$SiO$_4$ olivine and blue Co$_2$SiO$_4$ olivine are included in the CPMA Classification of the Mixed Metal Oxide Inorganic Coloured Pigments (CPMA-5-45-3 and CPMA-5-08-2) [1]. These compounds can be used as ceramic dyes. They are dissolved in glazes (as phosphates and borates). The formation of solid solutions with Mg(II) decreases the high content of nickel or cobalt in them and makes these materials less hazardous. The violet Co$_2$SiO$_4$ olivine pigment turns into deep blue in glazes [2].

In both Ni$_2$SiO$_4$ and Co$_2$SiO$_4$ compounds, the olivine structure is stable at atmospheric pressure. White Mg$_2$SiO$_4$ also crystallizes in this structure. Olivine structure presents an orthorhombic symmetry, std. S. G.: Pnma (nº 62), Z = 4, with std. cell 10.1173(5), 5.9125(4), 4.7277(5), in Ni$_2$SiO$_4$ [ICSD-35675], 10.2864(1), 5.9872(1), 4.7785(1), in Co$_2$SiO$_4$ [ICSD-260092] and 10.1989(2), 5.9812(6), 4.7561(2), in Mg$_2$SiO$_4$ [ICSD-242067] [3]. Their unit cell parameters are in accordance with the M(II) ionic radios M = Ni, Co and Mg, r(Ni^{2+}) < r(Mg^{2+}) < r(Co^{2+}). The variation of cell dimensions and interatomic distances with the ionic radius ratio r(M^{2+})/r(Si^{4+}) is not lineal. Mg$_2$SiO$_4$ olivine deviates significantly from the other olivine transition metals. The ionicity is higher in Mg^{2+} ions than in Ni^{2+}, Co^{2+}, Mn^{2+} and Fe^{2+} ions and it seems to be correlated to that deviation [4]. Two octahedral positions are occupied by M(II) ions in the olivine structure. M1 occupies the 4a site (special position with (0, 0, 0) fractional coordinates), M2, Si1, O1 and O2 occupy 4c sites (special position with (x, 0.25, z) fractional coordinates) and O3 occupies the 8d site (general position with (x, y, z) fractional coordinates). The atomic charge of the M2 site is larger than that of the M1 site. The M2 site probably has a more ionic character than the M1 site in the olivine structure [4].

Fig. 1 shows the unit cell of the olivine structure. It shows chains of M1O$_6$ octahedral in the b direction with shared opposite edges and trimers of octahedral M2O$_6$-M1O$_6$-M2O$_6$ with four oxygens in two opposite edges from M1O$_6$ shared with each M2O$_6$. The trimer containing M1 in the centre of the unit cell can be seen in Fig. 1. The axis of this trimer is located in a direction that is very close to the (110) plane. All the oxygens in the olivine structure are in tetrahedral coordination to three divalent cations and to one tetravalent silicon. SiO$_4$ tetrahedra are isolated, oxygens are not shared between tetrahedra. The structure was drawn with the Studio program [5–7].
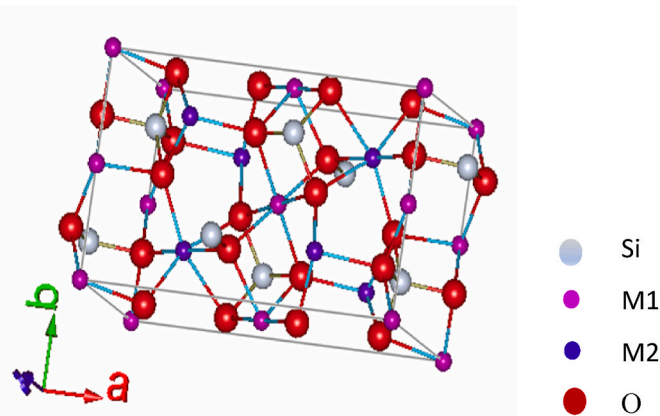
Fig. 1. Unit cell of the olivine structure.

A preference of transition metal ion for the M1 site is reported when $Mg_xNi_{2-x}SiO_4$ or $Mg_xCo_{2-x}SiO_4$ solid solutions with an olivine structure are formed. The cation ordering particularly influences the longest axis (a-axis in the std. cell). The M1 site is smaller and more distorted than the M2 site. The divalent cations are distributed in both M1 and M2 sites and the preference of Ni^{2+} or Co^{2+} ions for the M1 site is explained by the more covalent bonding provided by the d-orbitals of the transition metals and the p-orbitals of oxygen. The Mg^{2+} ions without electrons in d orbitals prefer the more ionic M2 site [8,9]. The cationic order between M1 and M2 sites is detected with positive deviations from the linear variation of the unit cell parameters [10]. The degree of site preference is higher in $(Ni, Mg)_2SiO_4$ than in $(Co, Mg)_2SiO_4$ [11].

The variation of the lattice parameters in Ni_2SiO_4–Co_2SiO_4 solid solutions with an olivine structure shows deviations of Vegard's law (deviations of the linear variation) and evidences the preferences of Ni^{2+} ion for the M1 octahedral site and Co^{2+} ion for the M2 octahedral site [12]. However, in another study, the linear variation of the lattice parameters and vibrational frequencies suggests that the mixing of α-Co_2SiO_4 and α-Ni_2SiO_4 is nearly ideal, and both Co^{2+} and Ni^{2+} in $(Co, Ni)_2SiO_4$ are distributed randomly in the M1 and M2 sites [13]. The results in [12,13] are contradictory and might be related to the thermal treatment of the samples at 1200 °C in [12] and between 1380 and 1440 °C in [13]. Mixtures of Co_3O_4, NiO and SiO_2 were used in both. The bibliography includes structural information about these solid solutions and although the colour green and blue of the Ni_2SiO_4 and Co_2SiO_4 compounds are reported [2], as far as we know, no information about the colour of these solid solutions has been published. In the case of the dark violet Co_2SiO_4 compound (prepared from a mixture of CoO and SiO_2 fired at 1400 °C for 48 h), the increase of unit cell parameters with a temperature between 51 and 300 K can be fitted to a curve, but it shows abrupt changes at 50 K. Below this temperature the lattice parameter b is shortened abruptly, whereas c increases and a keeps constant. However, the resulting volume of the unit cell continues its smooth decrease and does not reflect this anomaly. This anomaly can be associated with the magnetic phase transition taking place at this temperature [14].

The olivine structure is related with the $Ni_3P_2O_8$ structure. In both structures all the divalent cations (M1 and M2) occupy octahedral sites and the atoms with the most covalent bond occupy tetrahedral sites (SiO_4 and PO_4). The $Ni_3P_2O_8$ structure is less compact than the olivine structure and the coordination of the oxygens is lower (C.N.(O1, O2, O3) = 3, C.N.(O4) = 4) than in the olivine structure (C.N.(O) = 4). The incorporation of Co(II) in the $Ni_3P_2O_8$ structure decreases the yellow amount and increases the red amount. Yellow, beige, pink and red materials with a $Ni_3P_2O_8$ structure can be obtained from $Co_xNi_{3-x}P_2O_8$ (x ≤ 1.0) solid solutions between 800 and 1200 °C. The colour of these materials at these temperatures is in accordance with the position of the Ni^{2+} and Co^{2+} electronic transition bands in octahedral sites [15].

$Ni_3P_2O_8$ crystallizes in the monoclinic system with space group P 2_1/c (n° 14), a = 5.8310(1) Å, b = 4.6978(1) Å, c = 10.1098(3) Å, β = 91.129 (2)° and Z = 2 (ICSD-281705) [3]. Fractional coordinates of cations in olivine (x_o, y_o, z_o) are approximately equal to fractional coordinates in the $Ni_3P_2O_8$ structure (x_N, y_N, z_N), with a different order [(x_N, y_N, z_N) ~ (y_o, z_o, x_o) for Si^{4+}, P^{5+} and $M2^{2+}$] except for the cation in the M1 site with multiplicity 4 in the olivine (4a site, std. S.G.: Pnma) and 2 in the Ni (II) orthophosphate structure (2a site, S.G.: P 2_1/c). The unit cell in the olivine structure includes 8 M^{2+} (4 M1 and 4 M2), 4 Si^{4+} and 16 O^{2-} and in the Ni(II) orthophosphate structure 6 Ni^{2+} (2M1 and 4 M2), 4 P^{5+} and 16 O^{2-}. So, in the $Ni_3P_2O_8$ structure there are channels without atoms and the olivine structure is more compact.

The colour is modified by the changes in the bond strength. In compounds with shorter M − O distances, the ligand field strength increases and the electronic transition bands of cations appear at a smaller wavenumber in spectra. Displacements of these bands are not linear in accordance with the variation of the energies of the electronic transitions with the ligand field strength (Tanabe-Sugano diagrams). Mean M − O distances in Ni_2SiO_4 and Co_2SiO_4 with olivine structure are 2.090(2) and 2.126(2) Å, respectively (Ni1–O = 2.080(2), Ni2–O = 2.099(2); Co1–O = 2.116(2), Co2–O = 2.136(2)), while in $Ni_3P_2O_8$ and $Co_3P_2O_8$ with $Ni_3P_2O_8$ structure, they are 2.076(2) and 2.115(2) (Ni1–O = 2.075 (2), Ni2–O = 2.077(2); Co1–O = 2.001(2), Co2–O = 2.229(2))), with octahedral coordination in all of them. The smaller covalence of the Si–O bond in relation to the P–O bond lengthens the mean Ni–O and Co–O bonds and decreases the difference of Co1–O and Co2–O bonds. Considering the colourations obtained from $Co_xNi_{3-x}P_2O_8$ (x ≤ 1.0) solid solutions, it seems possible to obtain shades of pink or red from compositions with olivine structure. $Co_xNi_{3-x}P_2O_8$ (x ≥ 2.5) compositions develop the stable $Co_3P_2O_8$ structure (with pentacoordinate Co1 and octahedral Co2) and purple colourations are obtained [15]. Purple and violet colours are also obtained when the stable $Co_3P_2O_8$ structure is developed in $Mg_xCo_{3-x}P_2O_8$ (0 ≤ x ≤ 3) solid solutions. These colourations are kept at 1000 °C and at 1200 °C when x ≥ 1.5. The colour of $Mg_2CoP_2O_8$ composition is comparable to the purple $Co_3P_2O_8$ compound at 1200 °C [16]. So, the partial substitution of Ni(II) and Co(II) ions by Mg(II) ions with a lower amount of hazardous ions than in $M_3P_2O_8$ (M = Ni, Co) compositions might be obtained.

This study has three aims. The first aim is to investigate the possible formation of $MgCo_xNi_{1-x}SiO_4$ (0.0 ≤ x ≤ 1.0) solid solutions with olivine structure via the chemical coprecipitation method and to try to obtain materials with a smaller M(II) (M = Co, Ni) amount than Co_2SiO_4 and Ni_2SiO_4 compounds. The colour of these materials will be compared with that obtained from other compounds and powdered compositions containing Co(II) in order to explain the reason for the pink or red colour in some compositions and the blue o violet colour in other compositions, the second aim. And the third goal is to obtain materials of a glazed colour palette from dark green (with a higher Ni(II) amount than a Co(II) amount) to dark blue (with a higher Co(II) amount than a Ni(II) amount).

2. Experimental

$MgCo_xNi_{1-x}SiO_4$ (0 ≤ x ≤ 1) compositions were synthesized from colloidal SiO_2 (Scharlau), $MgCl_2·6H_2O$ (Scharlau, extra pure), Ni $(NO_3)_2·6H_2O$ (Acros Organic, 99%) and $Co(NO_3)_2·6H_2O$ (Acros Organic, 99%) via the chemical co-precipitation method.

Suspensions were prepared mixing the stoichiometric amount of SiO_2 with water. Then the stoichiometric amounts of $MgCl_2·6H_2O$, Ni $(NO_3)_2·6H_2O$ and $Co(NO_3)_2·6H_2O$ were added to these suspensions in continuous agitation. The coloured suspensions obtained were vigorously stirred for 20 h at room temperature. Then, an ammonia aqueous solution (Panreac, 25%) was added with continuous stirring until reaching pH = 10. In these conditions, the solid amount increased and the colour of the suspensions changed. The colour of the suspensions, before the addition of the ammonia solution, pH = 5–6, is green in x =

0.0 (due to the dissolution of the green Ni(NO$_3$)$_2$·6H$_2$O), red in x = 1.0 (due to the dissolution of the red Co(NO$_3$)$_2$·6H$_2$O) and mixed green-red in intermediate compositions. At pH = 10, green suspensions were obtained in all of compositions. The materials obtained were dried in a stove at 65 °C to evacuate the water only. The Si:Mg:Ni:Co molar ratio of the starting materials was preserved in this process. Green colloidal gels, solid material blocks formed by the physical bonding of particles with solvent retention were obtained. The colloidal gels were manually ground in an agate mortar to reduce the size of blocks of material and fired at 300, 600, 800, 1000 and 1200 ºC for 6 h at each temperature.

The development of the crystalline phases at different temperatures was studied by XRD. The resulting materials were examined using a Panalytical X-ray diffractometer (Malvern Panalytical, Almelo, The Netherlands) with CuK$_\alpha$ radiation. The unit cell parameters and interatomic distances in the developed structures were determined to investigate the possible formation of solid solutions under these synthesis conditions. A structure profile refinement was carried out via the Rietveld method (Fullprof.2k computer program) [5–7]. Diffraction patterns ranging between 6 and 110° (2θ) were collected employing monochromatic CuK$_\alpha$ radiation, a step size of 0.02° (2θ) and a sampling time of 10 s. The initial structural information of MgNiSiO$_4$ and MgCoSiO$_4$ compounds was taken from the Inorganic Crystal Structure Database [3]. This database includes standard cell, standard space group, fractional atomic coordinates and other information on crystalline phases found in the literature.

The Co(II) and Ni(II) sites and the transfer charge bands in the samples were studied by UV–vis–NIR spectroscopy (diffuse reflectance). The ultraviolet visible near infrared (UV–vis–NIR) spectra in the 200–2500 nm range was obtained using a Jasco V-670 spectrophotometer. To test the colour developed in glazes, the compositions fired at 1200 °C were 2% weight enamelled with a commercial glaze (SiO$_2$–Al$_2$O$_3$ – PbO–Na$_2$O – CaO glaze) onto commercial ceramic biscuits. Many pigments were dissolved in this glaze. The colour of the material is lost or change when this happens. Glazed tiles were fired for 15 min at 1065 °C and subsequently obtained their UV–vis–NIR spectra.

The CIEL*a*b* colour parameters on the fired samples - L* is the lightness axis (black (0) → white (100)), a* is the green (−) → red (+) axis, and b* is the blue (−) → yellow (+) axis [17] - were obtained with an X-Rite spectrophotometer (SP60, standard illuminant D65, a 10° observer, and a reference sample of MgO). The measurements were performed on powdered samples and on glazed tiles. Chroma (C* = $\sqrt{[(a*)^2 + (b*)^2]}$) and tone (H* = tg^{-1}(b*/a*)) were calculated from measure values of a* and b*. Chroma is the attribute that expresses the purity of a colour. Tone (synonym for hue, color, shade and tint) is the dominant wavelength of light that a person can see (yellow, red, blue, green, etc.). Mixing a pure hue with other colour reduces its purity and lowers its chroma. Images of samples at 15,000 magnification were obtained by scanning electron microscopy (JEOL-6610LV). The Cellpose image analysis program [18] was used to identify the particles. The image resulting from this identification is a mask image where the pixels belonging to the same particle have the same color. To measure the particle size, the Morpholibj [19] plugin of the FIJI program has been used.

3. Results and discussion

Table 1 shows the evolution of the crystalline phases with temperature in MgCo$_x$Ni$_{1-x}$SiO$_4$ (0 ≤ x ≤ 1.0) compositions and this evolution is shown for x = 0.25 and x = 0.75 compositions in Fig. 2. At 800 °C, the olivine crystalline phase is developed. Small amounts of NiO and MgSiO$_3$ are detected together with the olivine phase when x ≤ 0.5 and Co$_3$O$_4$ and MgSiO$_3$ is detected when x > 0.5. The amount of these minor crystalline phases decreases with temperature. At 1200 °C, the olivine amount is higher than 90% in all of the compositions and olivine is the only crystalline phase when x > 0.5.

Table 1
Crystalline phases in the MgCo$_x$Ni$_{1-x}$SiO$_4$ (0.0 ≤ x ≤ 1.0) compositions.

	800 °C	1000 °C	1200 °C
x = 0.00	O(m), N (m), M (w)	O(s), N (m), M (m)	O(s), N (w)
x = 0.25	O(s), N (w), M (m)	O(s), N (w), M(w)	O(s), N (vw)
x = 0.50	O(s), M(w)	O(s), N(vw)	O(s), N (vw)
x = 0.75	O(s), C (w), M (w)	O(s)	O(s)
x = 1.00	O(s), C (m), M (w)	O(s), C (vw)	O(s)

Crystalline phases: O = olivine, N = MO (M = Ni, Co), C = Co$_3$O$_4$, M = MgSiO$_3$.
Diffraction peak intensity: s = strong, m = medium, w = weak, vw = very weak.

From compositions fired at 1200 °C, the unit cell parameters, interatomic distances and M(II) ion (M = Mg, Ni, Co) occupation in M1 and M2 sites were obtained with the diffraction profile refinement by the Rietveld method. Fig. 3 shows graphical results of the olivine structure profile refinement carried out via the Rietveld method in MgCo$_x$Ni$_{1-x}$SiO$_4$ with x = 0.0, 0.5 and 1.0 compositions. Unit cell parameters and volume in olivine structure obtained from MgCo$_x$Ni$_{1-x}$SiO$_4$ (0.0 ≤ x ≤ 1.0) compositions fired at 1200 °C are shown in Table 2. The unit cell parameters in MgNiSiO$_4$ and MgCoSiO$_4$ compounds with the olivine structure obtained in this study are in accordance with the values in the literature [8,9]. Table 2 includes these values. Increasing the unit cell parameters with x is consistent with the replacement of the Ni(II) ion by the larger Co(II) ion and that confirms the formation of olivine solid solutions. The variation of the unit cell parameters with x is linear according to Vegard's law (Fig. 4). Thus, the Co(II) and Ni(II) are randomly distributed in the MgCo$_x$Ni$_{1-x}$SiO$_4$ (0.0 ≤ x ≤ 1.0) solid solutions with the olivine structure at 1200 °C. These results are in accordance with the random distribution of Co(II) and Ni(II) ions in the system Ni$_2$SiO$_4$–Co$_2$SiO$_4$ at 1380–1440 °C published by Lin [13]. The linear variation of olivine unit cell parameters in our study about MgCo$_x$Ni$_{1-x}$SiO$_4$ (0.0 ≤ x ≤ 1.0) solid solutions fired at 1200 °C doesn't evidence the site preferences of Ni(II) and Co(II) ions in the M1 and M2 sites in the olivine structure obtained by Zahn and Schreiter in Ni$_2$SiO$_4$–Co$_2$SiO$_4$ solid solutions at 1200 °C with deviations of Vegard's law [12].

The substitution of Ni(II) ions by the larger Co(II) ions increases all of the M1-O and M2-O distances (Table 3) and decreases the Si–O distances (Table 4). It seems that the covalence in the Si–O bond increases with x (with the cobalt amount). Fig. 5 shows the linear variation of the average M1-O, M2-O and Si–O distances with x. The increase in M1-O distances is larger than in the M2-O distances. This fact is in accordance with a higher occupation of M1 by Co(II) and Ni(II) ions than by Mg(II) ions and with the degree of site preference being higher in MgNiSiO$_4$ than in MgCoSiO$_4$ [11].

Due to the similar scattering factor of the Ni(II) and Co(II) ions, they are undistinguishable and it is not possible to refine the occupation in each position as an independent variable from Ni(II) and Co(II). The deviation of linearity of the variation of unit cell parameters with x allows one to establish the possible preference of one of these two ions by a site in the structure when solid solutions are formed. In the conditions of our study, no preferences between Ni(II) and Co(II) were detected and the occupation of these ions was determined using only one variable considering different values because of the stoichiometry of the composition. The different scattering factor of the Mg(II) ion makes it possible to refine its occupation considering that the occupation of (Ni (II)+Co(II)) + occupation of Mg(II) is 1.0. Fig. 6 shows the variation of the occupation of Co(II) and Mg(II) ions with a composition in M1 and M2 octahedral sites of olivine structure obtained in MgCo$_x$Ni$_{1-x}$SiO$_4$ (0 ≤ x ≤ 1.0) solid solutions. A slight deviation of the linear variation is detected in the Co(II) occupation. Experimental values are compared with the random distribution. In accordance with the same multiplicity of the two sites, a random distribution of the Mg(II) ions between the M1 and M2 sites corresponded to a ratio of 1/2 in each position. Because the magnesium amount is the same in all of samples, this random
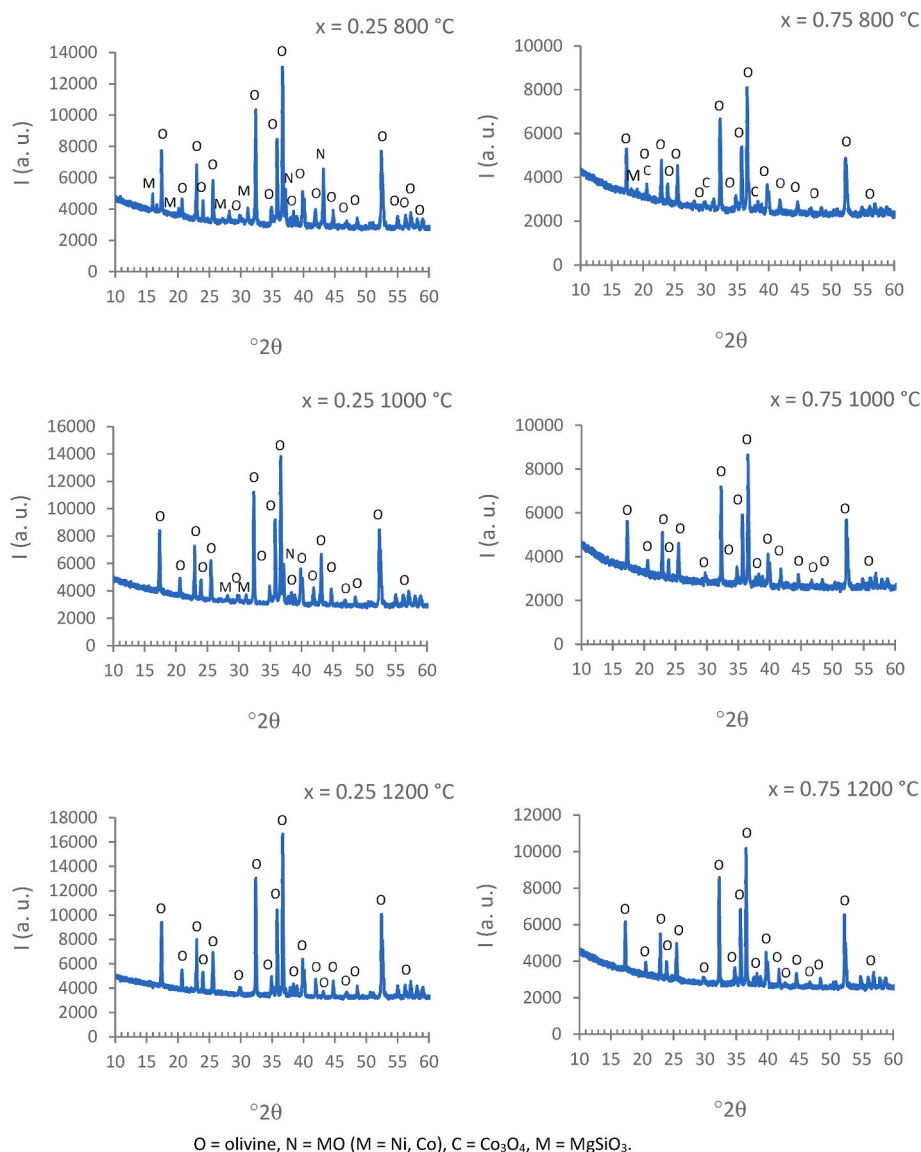
O = olivine, N = MO (M = Ni, Co), C = Co_3O_4, M = $MgSiO_3$.

Fig. 2. Evolution of crystalline phases in $MgCo_{0.25}Ni_{0.75}SiO_4$ and $MgCo_{0.75}Ni_{0.25}SiO_4$ compositions.

occupation is constant in all of the compositions. The change in the random distribution of Co(II) ion from 0.0 to 0.5 is due to the variation of the total cobalt amount in the composition (from 0.0 to 1.0). The occupation of Co(II) ions in M1 (4a) sites is obtained at a higher level than in M2 (4c) sites, considering a random distribution of Co(II) and Ni (II) ions in each site at 1200 °C (linear variation of unit cell parameters with a composition at 1200 °C). These results are in accordance with a preference of transition metal ion for the M1 site reported when $Mg_xNi_{2-x}SiO_4$ or $Mg_xCo_{2-x}SiO_4$ solid solutions with olivine structure are formed [10,11] and there is a higher degree of site preference in (Ni, Mg)$_2SiO_4$ than in (Co, Mg)$_2SiO_4$ [11].

Fig. 7 shows the UV–vis–NIR spectra of the $MgNiSiO_4$ composition (x = 0.0) fired at 800, 1000 and 1200 °C obtained in this study. Spectra of $Ni_3P_2O_8$ fired at 1000 °C and $NH_4[NiPO_4]\cdot H_2O$ compounds obtained by our group in previous studies are also included [15,20]. The three bands observed in experimental spectra of this composition (x = 0.0) can be assigned to the electronic transition bands of octahedral Ni(II). The first transition, $^3A_2 \rightarrow {}^3T_2(F)$, appears between 1000 and 1300 nm with a maximum at 1150 nm. The second transition, $^3A_2 \rightarrow {}^3T_1(F)$, appears between 600 and 900 nm with a maximum at 725 nm. And the third transition, $^3A_2 \rightarrow {}^3T_1(P)$, appears between 350 and 525 nm with a

maximum at 410 nm. These bands appear at slightly lower wavelengths (higher energy) in the $MgNiSiO_4$ composition than in the $Ni_3P_2O_8$ and $NH_4[NiPO_4]\cdot H_2O$ compounds. In the $MgNiSiO_4$ composition, a lower covalence of the Ni–O bond (octahedral NiO_6) (with the nephelauxetic ratio $\beta = B'/B$ approximately 0.85) is obtained than in $NH_4[NiPO_4]\cdot H_2O$ ($\beta = 0.81$) and $Ni_3P_2O_8$ ($\beta = 0.73$) compounds. B' is the B Racah experimental parameter obtained from the spectra for spin allowed bands, and B is the B Racah parameter for the free Ni(II) ion. This lower covalence in Ni–O bond from $MgNiSiO_4$ agrees with the longer mean M – O distance in this compound. In $MgNiSiO_4$, mean M – O is 2.102(2) Å (average M1-O = 2.087(1) Å and average M2-O = 2.117(2) Å) with M = Mg, Ni. In $NH_4[NiPO_4]\cdot H_2O$, mean Ni–O = 2.09(5) Å [18] and in $Ni_3P_2O_8$, mean Ni–O = 2.098(2) Å (average Ni1–O = 2.079(2) Å and average Ni2–O = 2.117(2) Å) [15].

Fig. 8 shows the UV–vis–NIR spectra of the $MgCoSiO_4$ composition (x = 1.0) fired at 800, 1000 and 1200 °C obtained in this study and the one of the $NH_4[CoPO_4]\cdot H_2O$ compound [20]. At 800 °C, the strong absorbance in all the wavelengths can be associated with the presence of Co_3O_4 detected by DRX. At 1000 and 1200 °C, the three bands observed in experimental spectra of this composition (x = 1.0) can be assigned to electronic transition bands of the octahedral Co(II). The first transition,
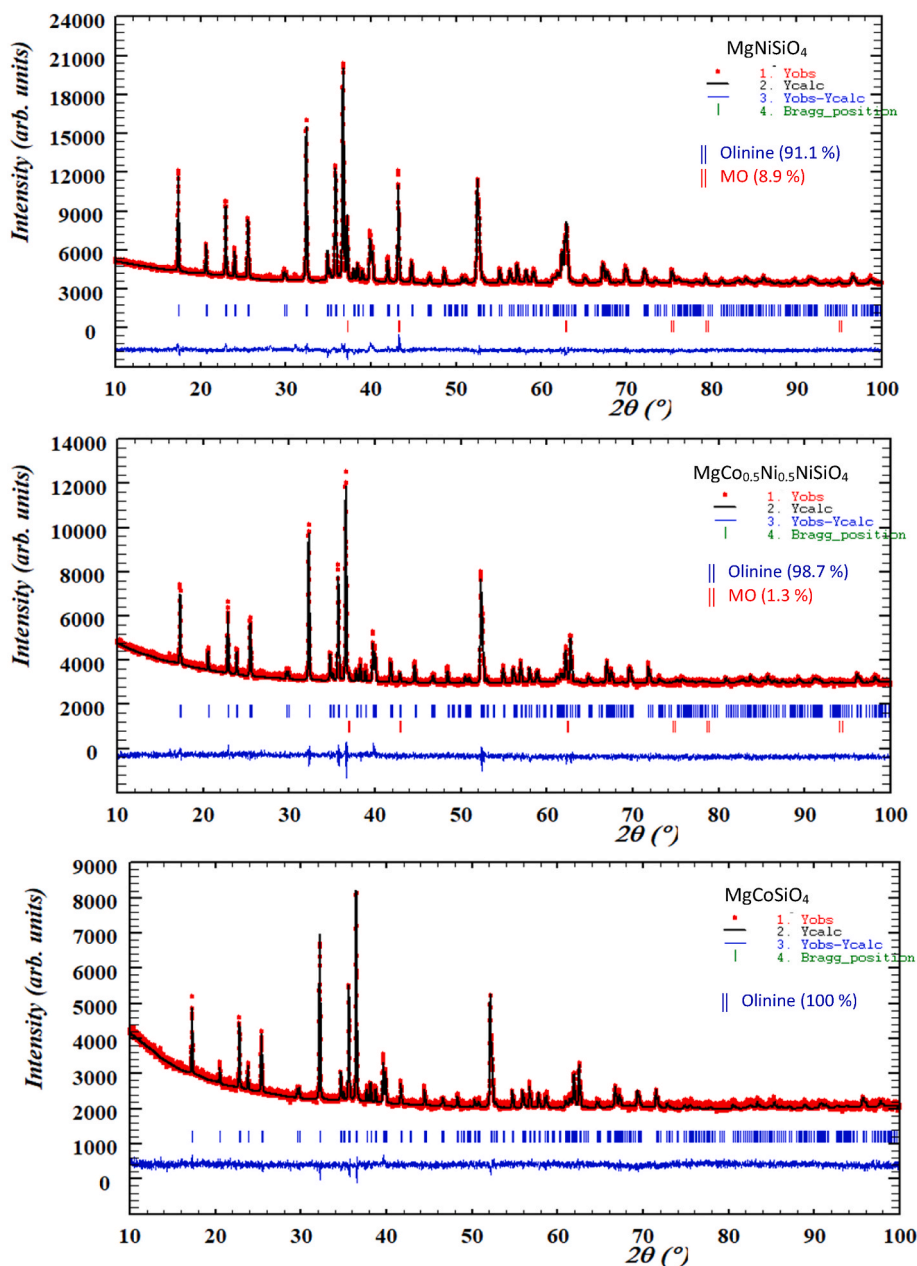
Fig. 3. The diffraction profile refinement by Rietveld's method from $MgCo_xNi_{1-x}SiO_4$ (x = 0.0, 0.5, 1.0) compositions fired at 1200 °C.

Table 2
Unit cell parameters in olivine structure obtained from $MgCo_xNi_{1-x}SiO_4$ ($0.0 \leq x \leq 1.0$) compositions fired at 1200 °C.

x	a (Å)	b (Å)	c (Å)	V (Å³)	Reference
0.00	10.187(1)	5.9467(7)	4.7396(5)	287.12(4)	[10]
0.00	10.18671(9)	5.94653(5)	4.73805(5)	287.010(5)	This study
0.25	10.2032(2)	5.95630(5)	4.74525(5)	288.384(5)	This study
0.50	10.2208(1)	5.96725(7)	4.75313(7)	289.894(5)	This study
0.75	10.2365(2)	5.97802(9)	4.76080(8)	291.331(6)	This study
1.00	10.2512(2)	5.98956(8)	4.76865(8)	292.795(8)	This study
1.00*	10.252(2)	5.9896(9)	4.7720(8)	293.0(1)	[11]

* Mg0.51Co0.49SiO4.

$^4T_1 \rightarrow {}^4T_2$, appears between 1050 and 1950 nm with two maxima at 1200 nm and 1550 nm. The second transition, $^4T_1 \rightarrow {}^4A_2$, appears between 700 and 850 nm with a maximum at 750 nm. And the third transition, $^4T_1 \rightarrow {}^4T_1(P)$, appears between 450 and 600 nm with three maxima at 470, 500 and 585 nm. In the $MgCoSiO_4$ compound, the first and second electronic transition bands appear at a higher wavelength (lower energy) than in the $NH_4[CoPO_4]\cdot H_2O$ compound and the third transition band appears at a slightly shorter wavelength (higher energy). Covalence of the Co–O bonds is obtained at a smaller level in the $MgCoSiO_4$ compound ($\beta = 0.94$) than in the $NH_4[CoPO_4]\cdot H_2O$ compound ($\beta = 0.81$). This is in accordance with the longer mean M − O distance in the $MgCoSiO_4$ compound in relation to the mean Co–O distance in $NH_4[CoPO_4]\cdot H_2O$. In $MgCoSiO_4$ the mean M − O distance is 2.126(2) Å (average M1-O = 2.117(1) Å and average M2-O = 2.136(2) Å) with M = Mg, Co (Table 3). In $NH_4[CoPO_4]\cdot H_2O$, the mean Co–O distance is 2.12(3) Å [20].

The position of the three transition bands in $MgCoSiO_4$ spectra (comparing values with the reference [21]) indicates a higher contribution of the Co(II) in M1 position in spectra. This is in accordance with the higher occupation of Co(II) in the M1 site than in the M2 site in olivine $MgCoSiO_4$ (Fig. 6). The blue olivine Co_2SiO_4 pigment contains
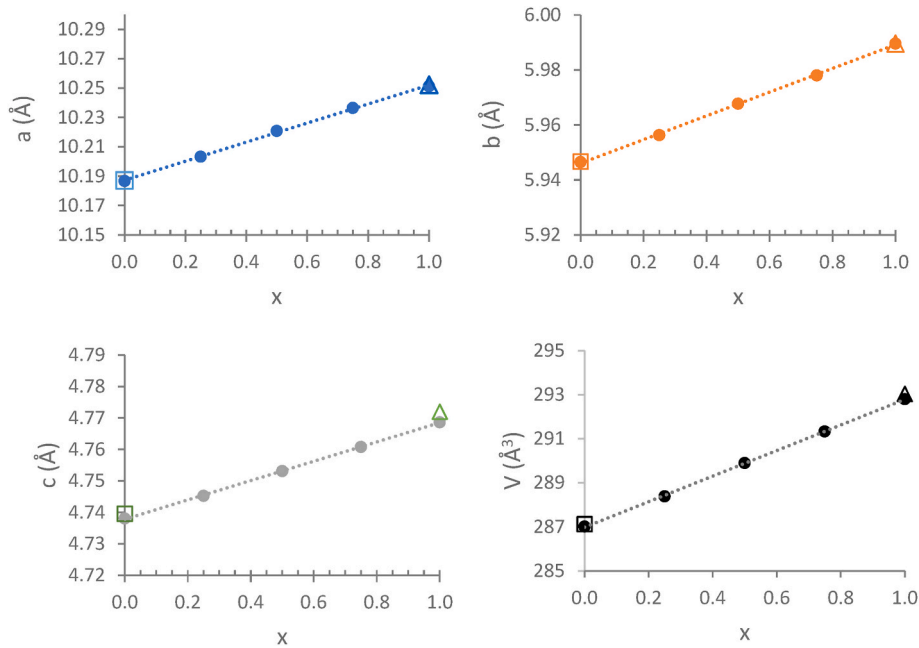
Fig. 4. Variation of unit cell parameters in olivine structure from MgCo$_x$Ni$_{1-x}$SiO$_4$ (0.0 ≤ x ≤ 1.0) compositions. Solid circles: Experimental values Squares: Values in Ref. 10 (MgNiSiO$_4$). Triangles: Values in Ref. 11 (MgCoSiO$_4$).

Table 3
M − O (M = Mg, Ni, Co) distances in olivine structure from MgCo$_x$Ni$_{1-x}$SiO$_4$ (0.0 ≤ x ≤ 1.0) compositions.

T (°C)	x	M1-O1 (x2) (Å)	M1-O2 (x2) (Å)	M1-O3 (x2) (Å)	Mean M1-O (Å)	M2-O1 (Å)	M2-O2 (Å)	M2-O3 (x2) (Å)	M2-O3 (x2) (Å)	Mean M2-O (Å)
1200	0.00	2.079(1)	2.067(1)	2.116(1)	2.087(1)	2.138(2)	2.047(2)	2.197(1)	2.062(1)	2.117(2)
1200	0.25	2.086(1)	2.069(1)	2.128(1)	2.094(1)	2.148(2)	2.051(2)	2.206(1)	2.059(1)	2.122(2)
1200	0.50	2.093(1)	2.072(1)	2.140(1)	2.102(1)	2.157(2)	2.056(2)	2.215(1)	2.057(2)	2.126(2)
1200	0.75	2.101(1)	2.075(1)	2.152(1)	2.109(1)	2.170(2)	2.058(2)	2.222(1)	2.057(2)	2.131(2)
1200	1.00	2.108(1)	2.079(1)	2.164(1)	2.117(1)	2.177(2)	2.065(2)	2.234(1)	2.053(2)	2.136(2)

Table 4
Si–O distances in olivine structure from MgCo$_x$Ni$_{1-x}$SiO$_4$ (0.0 ≤ x ≤ 1.0) compositions.

T (°C)	x	Si1–O1 (Å)	Si1–O2 (Å)	Si1–O3 (x2) (Å)	Mean Si1–O (Å)
1200	0.00	1.621(2)	1.654(2)	1.639(1)	1.638(2)
1200	0.25	1.620(2)	1.648(2)	1.636(1)	1.635(2)
1200	0.50	1.619(2)	1.644(2)	1.632(1)	1.632(2)
1200	0.75	1.618(2)	1.637(2)	1.630(2)	1.628(2)
1200	1.00	1.617(2)	1.631(2)	1.626(2)	1.625(2)

Co^{2+} in both M1 and M2 sites. For M1, the components of the first transition appear at 1812, 1587 and 1333 nm and components of the third transition appear at 580, 551, 526 and 493 nm. For M2, the components of the first transition are at 1205 and 1156 nm and components of the third transition are at 625, 513 and 474 nm. The second transition appears at 750 nm and it is due to M1 Co^{2+} and M2 Co^{2+} ions. Due to the greater distortion of the M2 site, the bands in the spectrum arising from the M2 Co^{2+} ions have a higher intensity than those from the M1 Co^{2+} [21]. The position of the third transition at slightly shorter wavelengths in pink MgCoSiO$_4$ than those in blue Co$_2$SiO$_4$ might be related to the different colour of these compounds.

Fig. 9 shows the UV–vis–NIR spectra of MgCo$_x$Ni$_{1-x}$SiO$_4$ (0 ≤ x ≤ 1.0) solid solutions at 600, 800, 1000 and 1200 °C and Table 5 shows the CIE L*a*b* parameters, chroma (C*) and tone (H*) of these compositions from raw materials at 1200 °C. Changes in the shape and the position of bands in spectra are in accordance with the crystalline phases developed in each composition. At 600 °C, when x = 0.0, bands are detected with
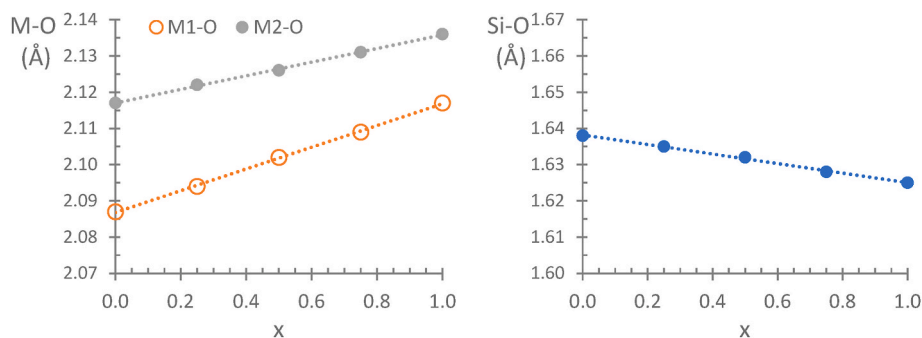

Fig. 5. Variation of average distances in olivine structure from MgCo$_x$Ni$_{1-x}$SiO$_4$ (0.0 ≤ x ≤ 1.0) compositions fired at 1200 °C.

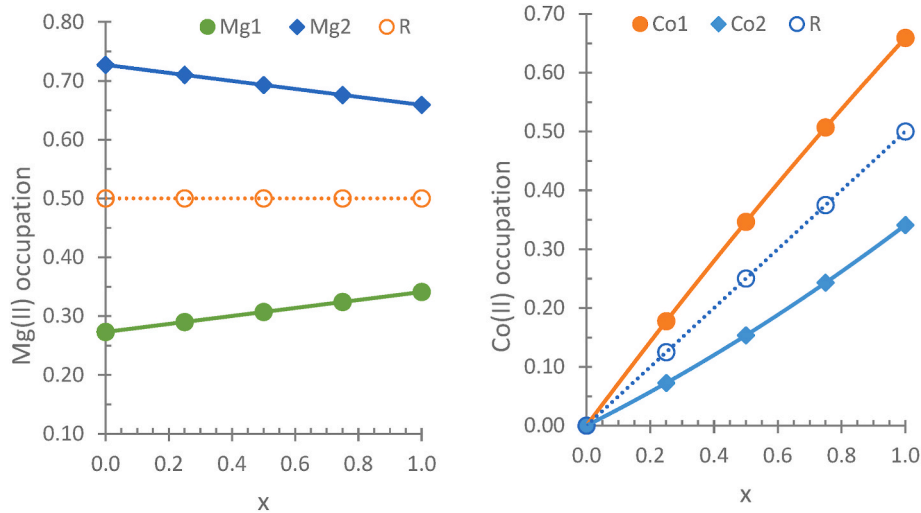**Fig. 6.** Occupation of Co(II) and Mg(II) ions with a composition in M1 and M2 octahedral sites of olivine structure from $MgCo_xNi_{1-x}SiO_4$ ($0.0 \leq x \leq 1.0$) compositions at 1200 °C. Co1, Mg1: Experimental occupation in octahedral M1 sites. Co2, Mg2: Experimental occupation in octahedral M2 sites. R: theoretical random occupation in octahedral M1 and M2 sites.
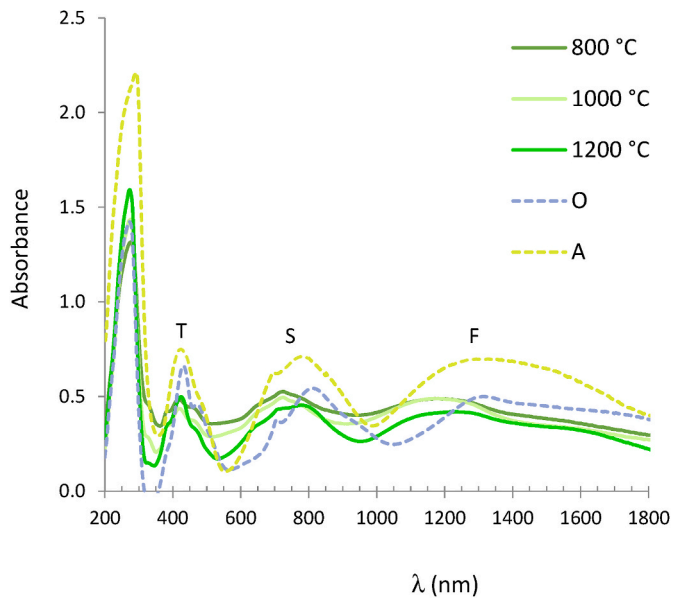

Fig. 7. UV–vis–NIR spectra of $MgNiSiO_4$ composition ($x = 0.0$) fired at 800 °C, 1000 °C and 1200 °C, $Ni_3P_2O_8$ fired at 1000 °C (O) and $NH_4[NiPO_4]\cdot H_2O$ (A). Ni(II) CN = 6: (F) $^3A_2 \rightarrow {}^3T_2(F)$, (S) $^3A_2 \rightarrow {}^3T_1(F)$, (T) $^3A_2 \rightarrow {}^3T_1(P)$.

Fig. 8. UV–vis–NIR spectra of $MgCoSiO_4$ ($x = 1.0$) compositions at 800 °C, 1000 °C and 1200 °C and $NH_4[CoiPO_4]\cdot H_2O$ (B). Co(II) CN = 6: (1) $^4T_1 \rightarrow {}^4T_2$, (2) $^4T_1 \rightarrow {}^4A_2$, (3) $^4T_1 \rightarrow {}^4T_1(P)$.

two maxima at this temperature due to the presence of octahedral Ni(II) ions in both olivine and NiO structures. At this temperature, grey colourations of compositions that contain cobalt ($x \neq 0$) are in accordance with the strong absorbance in all the wavelengths. At 800 °C, the strong absorbance is only obtained when $x > 0.5$ and it is associated with the presence of Co_3O_4 detected by DRX in these compositions. When $x \leq 0.5$ at 800 °C and in all compositions at 1000 and 1200 °C, the three absorption bands observed in experimental spectra can be assigned to octahedral Ni(II) and Co(II) ions in samples and the olivine structure is obtained as the major crystalline phase. At 1000 °C and 1200 °C, only small amounts of minor crystalline phases are detected together with the olivine crystalline phase and the colour of these solid solutions is pink when $x \neq 0$.

At 1000 °C and 1200 °C, the colour of the $MgCo_xNi_{1-x}SiO_4$ ($0.25 \leq x \leq 1.0$) solid solutions gradually changes with x, when the amount of Co(II) increases and the amount of Ni(II) decreases. The composition
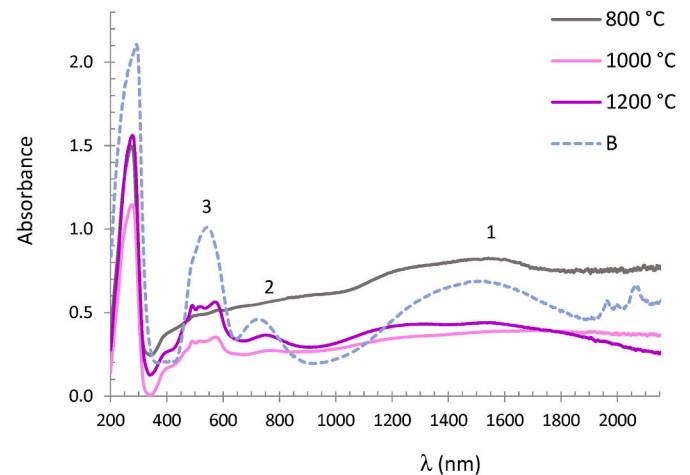
without cobalt ($x = 0.0$) is green and pink samples are obtained in compositions with cobalt ($x \neq 0.0$) at these temperatures. The pink colour of samples with $x > 0.0$ is due to the absorbance between 440 and 630 nm, assigned to the third transition band in octahedral Co(II), $^4T_1 \rightarrow {}^4T_1(P)$. The absorbance in this wavelengths range increases with x (Co(II) amount), the a* colour parameter (+, red amount) increases from +3.34 ($x = 0.25$) to +12.55 ($x = 1.00$) and the b* colour parameter (yellow amount (+) to blue amount (−)) decreases from +7.13 ($x = 0.25$) to −5.61 ($x = 1.00$). The variation of a* and b* colour parameters, chroma (C*) and tone (H*) in samples fired at 1200 °C is shown in Fig. 10. When x increases, the H* values are in accordance with the decrease of yellow amount ((+) b*) and in compositions with $x \geq 0.5$ values are into the red range (into 0–50° or 350–360°). The H* value about 120° in $MgNiSiO_4$ ($x = 0$) correspond to green colour and the H* value next to 60° to yellow colour. The increase of C* when x increases in compositions with $x \geq 0.5$ indicates an increase of the purity of the red colour. The C* value is higher when $x = 0$ ($MgNiSiO_4$) than when $x = 1$ ($MgCoSiO_4$). It might be related with the narrower bands in $MgNiSiO_4$ spectrum than in $MgCoSiO_4$ spectrum (Fig. 9 d). The $MgCo_xNi_{1-x}SiO_4$ ($0.0 \leq x \leq 1.0$) solid solutions are stable at 1200 °C and might be used as

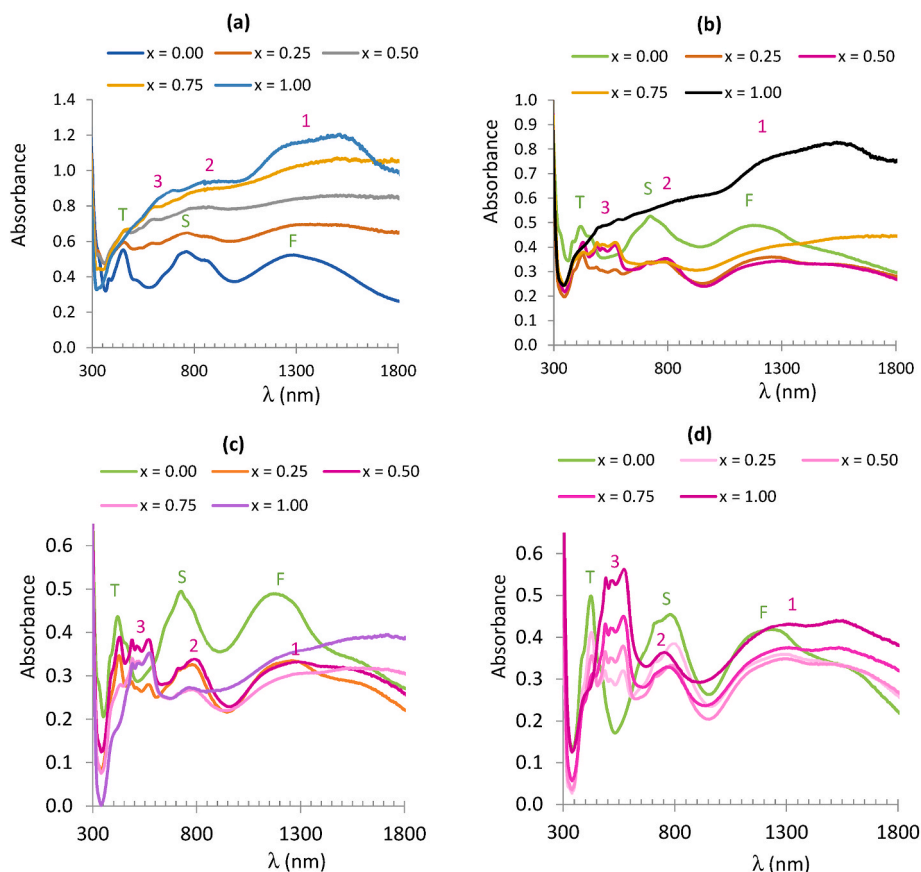**Fig. 9.** UV–vis–NIR spectra of $MgCo_xNi_{1-x}SiO_4$ ($0.0 \leq x \leq 1.0$) compositions at (a) 600 °C, (b) 800 °C, (c) 1000 °C and (d) 1200 °C. Ni(II) CN = 6: (F) $^3A_2 \rightarrow {}^3T_2$(F), (S) $^3A_2 \rightarrow {}^3T_1$(F), (T) $^3A_2 \rightarrow {}^3T_1$(P). Co(II) CN = 6: (1) $^4T_1 \rightarrow {}^4T_2$, (2) $^4T_1 \rightarrow {}^4A_2$, (3) $^4T_1 \rightarrow {}^4T_1$(P).

Table 5
CIE L*a*b* parameters, chroma (C*) and tone (H*) from $MgCo_xNi_{1-x}SiO_4$ ($0.0 \leq x \leq 1.0$) compositions.

x		Raw material	300 °C	600 °C	800 °C	1000 °C	1200 °C
0.00	L*	73.20	75.46	72.59	73.39	75.78	81.59
	a*	−24.70	−0.05	+0.02	−4.55	−5.28	−9.91
	b*	+14.27	+23.94	+17.30	+8.37	+7.86	+18.82
	C*	28.53	23.94	17.30	9.53	9.47	21.27
	H* (°)	149.99	90.12	89.98	118.52	123.89	117.77
	Colour	Green	Yellow	Greenish yellow	Green	Green	Green
0.25	L*	61.68	58.49	61.52	77.60	80.66	79.12
	a*	−14.74	−8.11	−0.82	+0.77	+1.58	+3.34
	b*	+6.64	−1.15	+3.13	+4.92	+5.85	+7.13
	C*	16.17	8.19	3.24	4.98	6.06	7.87
	H* (°)	155.75	188.07	104.68	81.10	74.88	64.90
	Colour	Green	Green	Greyish green	Beige	Beige	Pale Pink
0.50	L*	65.71	60.99	52.71	73.02	75.13	74.81
	a*	−8.40	−6.03	−2.03	+6.78	+7.16	+8.08
	b*	+4.77	−5.68	−2.19	+4.50	+4.78	+2.80
	C*	9.66	8.28	2.99	8.14	8.61	8.55
	H* (°)	150.41	223.29	227.17	33.57	33.73	19.11
	Colour	Green	Greenish blue	Grey	Pink	Pink	Pink
0.75	L*	71.95	62.56	51.39	73.66	76.88	72.06
	a*	−9.66	−6.34	−3.46	+5.34	+7.27	+10.25
	b*	+3.06	−9.11	−5.83	+1.95	+1.12	−1.42
	C*	10.13	11.10	6.78	5.68	7.36	10.35
	H* (°)	162.42	235.16	239.31	20.06	8.76	352.12
	Colour	Green	Blue	Bluish grey	Pink	Pink	Pink
1.00	L*	72.05	63.83	51.22	64.83	76.61	66.67
	a*	−9.31	−7.02	−4.24	−1.00	+7.61	+12.55
	b*	+3.87	−11.31	−9.20	−5.02	−4.94	−5.61
	C*	10.08	13.31	10.13	5.12	9.07	13.75
	H* (°)	157.43	238.17	245.26	258.73	327.01	335.92
	Colour	Green	Blue	Greyish blue	Greyish lilac	Lilac pink	Pink

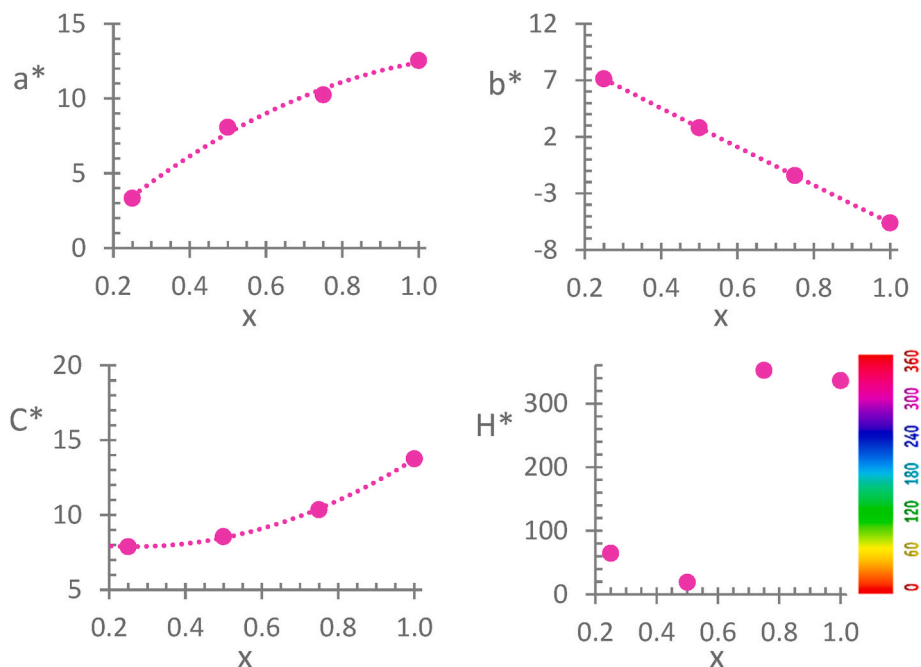**Fig. 10.** CIE L* a* b*, C* and H* from $MgCo_xNi_{1-x}SiO_4$ $(0.0 \leq x \leq 1.0)$ powdered compositions at 1200 °C.

yellowish green (x = 0.0) or pink (x > 0.0) paint pigments (Table 5). Fig. 11 shows the variation of the colour observed with composition and temperature in these compositions.

Fig. 12 shows images of $MgCo_xNi_{1-x}SiO_4$ powdered solid solutions fired at 1200 °C obtained by electron microscopy. The size of the particles is quite homogeneous about 0.5 μm and it increases slightly with x. Table 6 includes the average maximum diameter and the total number of measured particles for each composition.

Fig. 13 shows visible spectra of $MgCo_{0.25}Ni_{0.75}SiO_4$ (x = 0.25) and $MgCoSiO_4$ (x = 1.00) solid solutions with an olivine structure fired at 1200 °C compared with the $NH_4[CoPO_4] \cdot H_2O$ compound at 180 °C, the $Mg_{1.5}Co_{1.5}P_2O_8$ composition with the stable-$Co_3P_2O_8$ structure fired at 1200 °C, the $CoNi_2P_2O_8$ and $Co_2NiP_2O_8$ solid solutions with the $Ni_3P_2O_8$ structure fired at 1200 °C and $Co(NO_3)_2 \cdot 6H_2O$ used in the preparation of the pink olivine solid solutions. Because the Co(II) site changes in different structures and compositions, the colours pink, reddish, violet or purple observed in these materials are not in accordance to their total cobalt amount (%-weight: $MgCo_{0.25}Ni_{0.75}SiO_4$, 8.4% < $CoNi_2P_2O_8$, 16.1% < $Co(NO_3)_2 \cdot 6H_2O$, 20.2% < $Mg_{1.5}Co_{1.5}P_2O_8$, 28.1% < $NH_4[CoPO_4] \cdot H_2O$, 31.1% < $Co_2NiP_2O_8$, 32.2% < $MgCoSiO_4$, 33.6%). The great bandwidth in some spectra ($NH_4[CoPO_4] \cdot H_2O$, $MgCoSiO_4$) is in accordance with the high distortion of octahedra CoO_6 and makes it difficult to establish the position of the bands. Second and third electronic transition bands of octahedral Co(II) ion appear superimposed in some compositions ($Co_2NiP_2O_8$, $Mg_{1.5}Co_{1.5}P_2O_8$) and this increases the absorbance in 580–650 nm (blue colour observed).

The absorbance in the $MgCo_xNi_{1-x}SiO_4$ $(0.25 \leq x \leq 1.0)$ solid solutions with the olivine structure is smaller than in the other compositions and it increases with the cobalt amount (Fig. 9 (d)). In these olivine solid solutions, second and third transition bands of octahedral Co(II) ion appear separated at 1000 °C and 1200 °C. The presence of Ni(II) ions decreases the M1-O distances and the amount of Co(II) in the compositions, so the absorbance of the bands corresponding to octahedral Co(II) decreases and the pink colour is less intense than in the composition $MgCoSiO_4$.

Table 7 shows CIEL*a*b* colour parameters, chroma (C*), tone (H*), M − O distances (M = Co, Ni, Mg) and the colours observed in some powdered compositions with octahedral Co(II) for comparison with the results in this study. The pink colour of $MgCo_xNi_{1-x}SiO_4$ $(0.25 \leq x \leq 1.0)$

solid solutions fired at 1200 °C contains a smaller amount of red (positive a*) and blue (negative b*) than the violet $NH_4[CoPO_4] \cdot H_2O$ composition at 180 °C (Tables 5 and 7). Although red and reddish pink colours are obtained when a* >20 and pink is obtained when 10 < a* <20, a* = 41.83 in $NH_4[CoPO_4] \cdot H_2O$ compound. From information of M − O distances in structures with Co(II) ions only in octahedral sites, one might establish a limit value of 2.12 Å. This limit value explains the pink colour of $MgCo_xNi_{1-x}SiO_4$ $(0.25 \leq x \leq 1.0)$ solid solutions while Co_2SiO_4 is blue or violet. It can be extended to other compounds containing octahedral Co(II) ions. When the M − O distance is less than 2.12 Å, materials are yellow ($CoCrO_4$, Co–O: 2.065 Å, ICSD-23492), pink (in pink $Co(OH)_2$, Co–O: 2.117 Å, ICSD-257275) or red ($Co(NO_3)_2 \cdot 6H_2O$, Co–O: 2.078 Å, ICSD-9263), and when it is greater than this value, the colour of the material is blue, violet, purple or green (in violet $CoMoO_4$, Mean Co–O: 2.128 Å, ICSD-760022 and in green $CoBr_2$, Co–Br: 2.626 Å, ICSD-52364). The shorter distances might be associated with the yellow, pink and red colours in materials with Co(II). In the blue Co_2SiO_4 compound, the colour and bands in spectra are due to the Co(II) ions in the two octahedral positions in olivine structure and the mean Co–O distance is 2.126 Å (higher than the limit value). In the $MgCoSiO_4$ compound the total Co(II) amount is distributed approximately 2/3 in M1 (2.117 Å) and 1/3 in M2 (2.136 Å). The contribution to colour and bands in spectra is higher in the Co(II) in M1. In the pink $MgCo_xNi_{1-x}SiO_4$ $(0.25 \leq x \leq 1.00)$ solid solutions, the mean M1-O distance is between 2.094 Å and 2.117 Å, all of them being smaller than 2.12 Å (limit value). The a* colour parameter increases and b* colour parameter decreases with x in them (Fig. 10).

Fig. 14 shows the visible spectra and Table 8 CIE L* a* b* colour parameters, chroma (C*) and tone (H*) in glazed tiles prepared with 2% $MgCo_xNi_{1-x}SiO_4$ $(0.0 \leq x \leq 1.0)$ solid solutions fired at 1200 °C. Beige (x = 0.0); green $(0.0 < x \leq 0.5)$ and blue $(0.5 < x \leq 1.0)$ colours are obtained in enamelling samples. The absorbance at 490–550 nm (responsible for the colour observed in powdered pink solid solutions) is present when x > 0.0. A new band at 650 nm is observed in the enamelled samples when x > 0.0 (in all samples containing cobalt). This band can be assigned to tetrahedral Co(II) ion, $^4A_2 \rightarrow {}^4T_1$ (P) and is responsible for the blue component in the colour of the samples. The blue colour is the colour observed when x > 0.5. When $0.0 < x \leq 0.5$, the colour observed is green and seems due to both the strong absorbance between 450 and
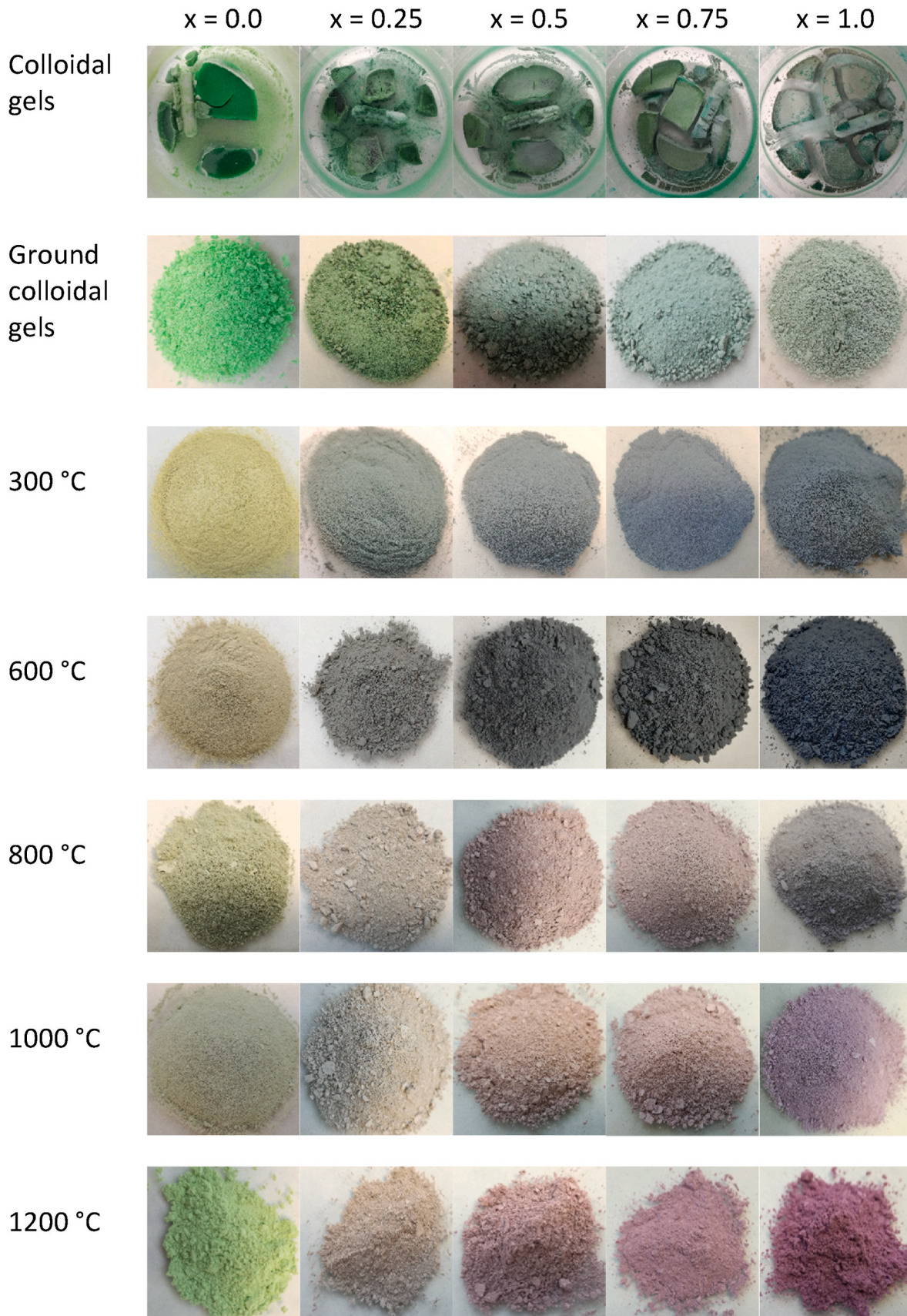
Fig. 11. The colour images of all the prepared samples (dried gels and fired MgCo$_x$Ni$_{1-x}$SiO$_4$ $0.0 \leq x \leq 1.0$ compositions). (For interpretation of the references to colour in this figure legend, the reader is referred to the Web version of this article).
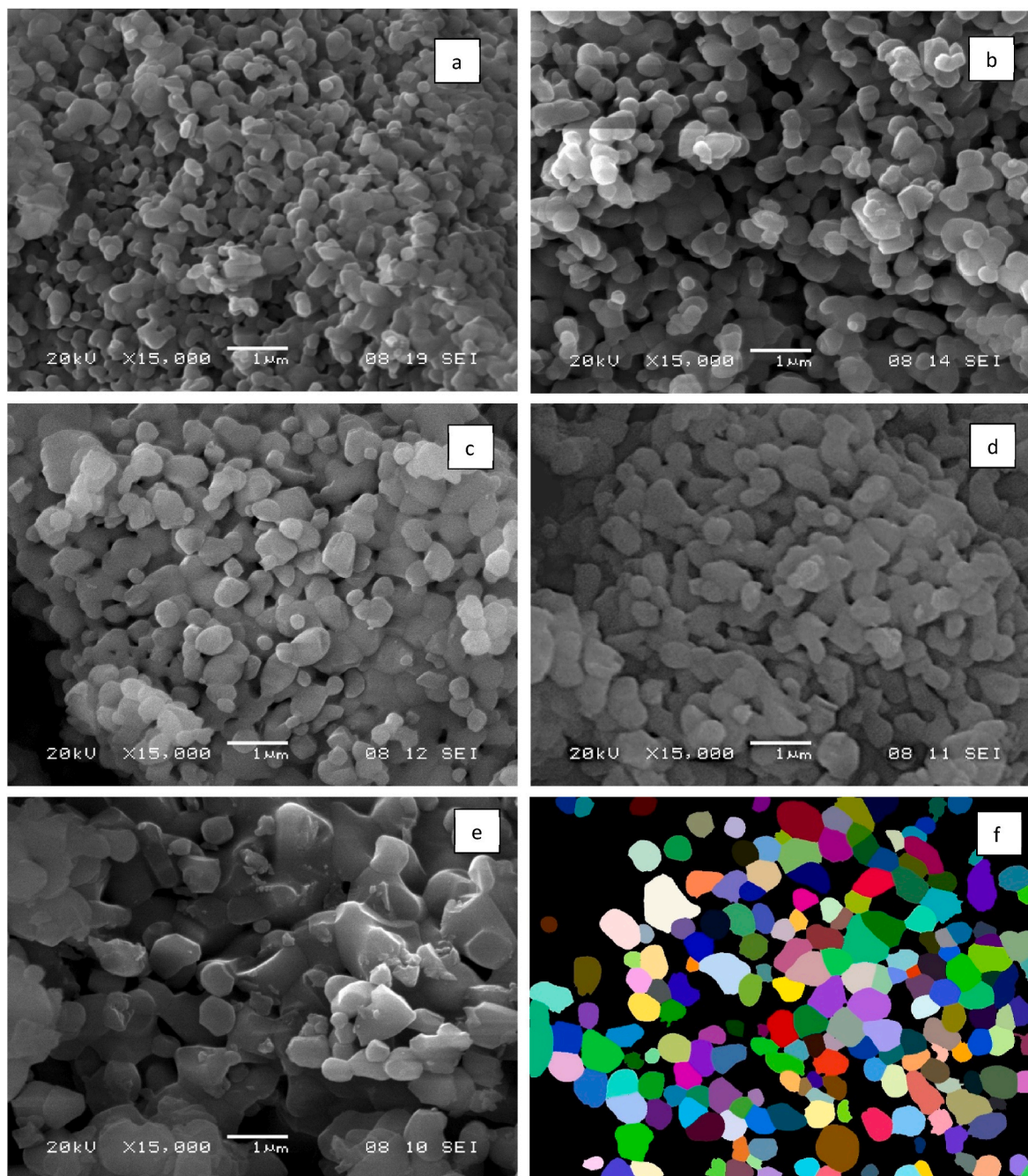
Fig. 12. SEM images of MgCo$_x$Ni$_{1-x}$SiO$_4$ compositions fired at 1200 °C, (a) x = 0.00, (b) x = 0.25, (c) x = 0.50, (d) x = 0.75, (e) x = 1.00 and (f) mask image from x = 0.75 composition.

Table 6
Average maximum diameter in MgCo$_x$Ni$_{1-x}$SiO$_4$ powdered solid solutions fired at 1200 °C.

x	Total number of measured particles	Average maximum diameter
0.00	686	0.353
0.25	507	0.415
0.50	394	0.461
0.75	277	0.562
1.00	351	0.699

700 nm, including the band at 650 nm assigned to tetrahedral Co(II), and that at 430 nm, including the band assigned to the third transition of octahedral Ni(II). The lower absorbance in $\lambda > 725$ nm than in $\lambda < 725$ nm is in accordance with the dissolution of the solid solutions in glazes. The second transition of octahedral Co(II) detected about 800 nm in powdered solid solutions and is indistinguishable from the strong absorbance between 500 and 700 nm in the enamelled MgCoSiO$_4$ composition. The decreases of the absorbance of band at this wavelength with the Ni(II) content make it possible to assign it only to the second transition band of octahedral Ni(II). This second transition band of octahedral Ni(II) can be observed but its absorbance is not comparable to the third transition of this ion. First transition bands of octahedral Ni (II) and Co(II) are poorly defined in enamelled samples. The pinhole defect due to loss of oxygen in some pigments with cobalt synthesized from oxides is not detected in the enamelling of samples because the Co$_3$O$_4$ compound is not present in powdered pink solid solutions at 1200 °C. So, these MgCo$_x$Ni$_{1-x}$SiO$_4$ ($0.0 \leq x \leq 1.0$) solid solutions fired at
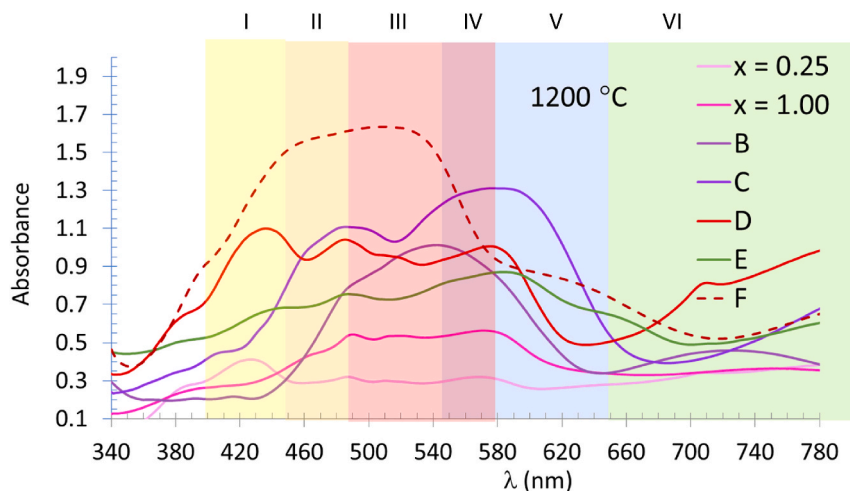
Colour observed, I: Yellow (400-450 nm), II: Orange (450-490 nm), III: Red (490-550 nm),
IV: Violet (550-580 nm), V: Blue (580-650 nm), VI: Green (650-800 nm).

Fig. 13. Visible spectra of pink $MgCo_{0.25}Ni_{0.75}SiO_4$ (x = 0.25) and $MgCoSiO_4$ (x = 1.00) solid solutions with an olivine structure fired at 1200 °C and some compounds including Co(II). B: $NH_4[CoPO_4] \cdot H_2O$ 180 °C (violet) [20], C: $Mg_{1.5}Co_{1.5}P_2O_8$ at 1200 °C (purple) [16], D: $CoNi_2P_2O_8$ at 1200 °C (red) [15], E: $Co_2NiP_2O_8$ at 1200 °C (violet) [15], F: $Co(NO_3)_2 \cdot 6H_2O$ (red). (For interpretation of the references to colour in this figure legend, the reader is referred to the Web version of this article).

Table 7
CIE L* a* b* colour parameters, chroma (C*), tone (H*), M − O distances and colours observed in some powdered compositions containing cobalt [15,16,20,22].

Composition	T (°C)	L*	a*	b*	C*	H* (°)	Mean M-O* distance (Å)	Colour observed
$NH_4[CoPO_4] \cdot H_2O$[a]	180	51.38	+41.83	- 34.16	42.20	352.36	2.12	Violet
$NH_4[Co_{0.8}Ni_{0.2}PO_4] \cdot H_2O$[a]	180	44.29	+31.31	- 12.12	33.57	338.84	2.11	Reddish pink
$NH_4[Co_{0.5}Ni_{0.5}PO_4] \cdot H_2O$[a]	180	53.91	+24.06	+1.73	24.12	4.11	2.10	Reddish pink
$NH_4[Co_{0.2}Ni_{0.8}PO_4] \cdot H_2O$[a]	180	68.13	+11.78	+17.82	21.36	56.53	2.09	Pink-beige
$Co_2P_2O_7$[b]	1200	34.84	+11.53	- 11.41	16.22	315.3	2.115 (2.040)	Intense violet
$Co_{1.6}Ni_{0.4}P_2O_7$[b]	1200	39.84	+5.55	+0.01	5.55	0.10	2.110 (2.042)	Greyish violet
$CoNiP_2O_7$[b]	1200	41.05	+3.99	+11.64	12.30	71.08	2.112 (2.040)	Reddish brown
$Co_{0.4}Ni_{1.6}P_2O_7$[b]	1200	59.62	+2.15	+27.42	27.50	85.52	2.123 (2.043)	Yellowish
$Co_2NiP_2O_8$[c and d]	1200	45.33	+6.26	+4.68	7.82	36.78	2.097 2.147 (2.054)	Violet
$Co_{1.5}Ni_{1.5}P_2O_8$[c]	1200	48.44	+14.98	- 9.62	17.80	327.29	2.087	Dark pink
$CoNi_2P_2O_8$[c]	1200	48.62	+20.35	+14.84	25.19	36.10	2.087	Red
$Co(NO_3)_2 \cdot 6H_2O$[e]	25	39.09	+22.60	+21.70	31.33	43.84	2.078	Red
$Mg_{1.5}Co_{1.5}P_2O_8$[d]	1200	36.24	+18.62	−18.33	26.13	315.45	2.131 (2.044)	Purple
Co_2SiO_4[f]	1200	45.67	+6.08	−24.95	25.68	283.70	2.116, 2.136	Violet-Blue
$MgCoSiO_4$[f]	1200	66.67	+12.55	- 5.61	13.75	355.92	2.117, 2.136	Pink

*Octahedral M − O distance, (M − O distance in CN = 5). Esd ≤0.04 in $NH_4[CoPO_4] \cdot H_2O$ structure and it is about 0.002 in the other structures.

[a] $NH_4[CoPO_4] \cdot H_2O$.

[b] $Co_2P_2O_7$.

[c] $Ni_3P_2O_8$.

[d] $Co_3P_2O_8$.

[e] $Co(NO_3)_2 \cdot 6H_2O$.

[f] Co_2SiO_4 structures.

1200 °C can be used in ceramic industry, decreasing the content of nickel and cobalt with respect to that existing in the Ni_2SiO_4 and Co_2SiO_4 compounds.

4. Conclusions

In this paper $MgCo_xNi_{1-x}SiO_4$ (0 ≤ x ≤ 1) solid solutions with the olivine structure were obtained via the chemical co-precipitation method in compositions fired at 1200 °C. These new materials, in the conditions of our study, show the Ni(II) and Co(II) cations randomly distributed. The solid solutions exhibit a linear variation of unit cell parameters with the Ni/Co contents x and the occupation of the Ni(II) and Co(II) ions in M1 (4a) sites was obtained at a higher level than in M2 (4c) sites, whereas the Mg(II) ions were found preferably occupying the

M2 site.

The composition without cobalt (x = 0.0) is green and the colour of the $MgCo_xNi_{1-x}SiO_4$ (0.25 ≤ x ≤ 1.00) solid solutions is pink at 1200 °C, the pink colour of solid solutions with cobalt being due to the absorbance between 440 and 630 nm, assigned to the third transition band in octahedral Co(II).

From the information of M − O distances in the structures containing Co(II) ions only in octahedral sites, a limit value of 2.12 Å was established to obtain pink or red materials, as for longer M − O distances the colour of materials is blue, violet or green.

When $MgCo_xNi_{1-x}SiO_4$ (0.0 ≤ x ≤ 1.0) solid solutions were dissolved in the commercial glaze tested, beige (x = 0.0), green (0.0 < x ≤ 0.5) and blue (0.5 < x ≤ 1.0) colours were obtained in enamelling samples, leading to the conclusion that $MgCo_xNi_{1-x}SiO_4$ (0.0 ≤ x ≤ 1.0) solid

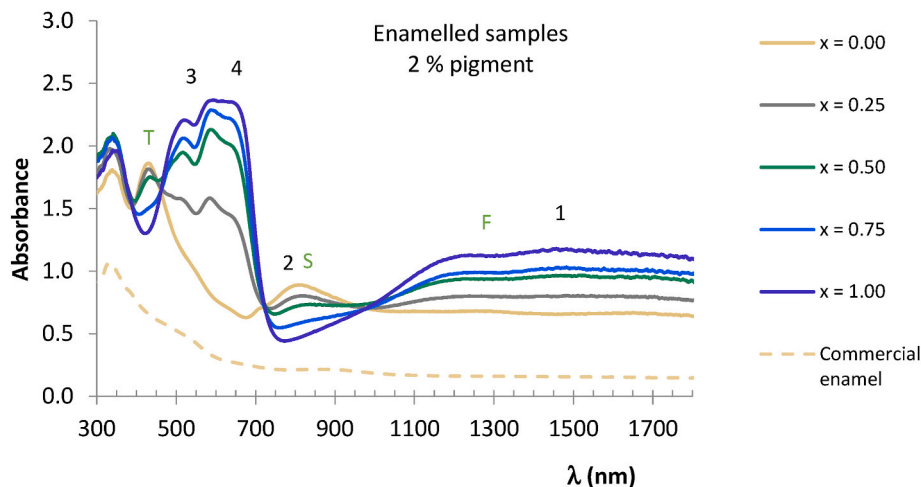**Fig. 14.** UV–vis–NIR spectra of enamelled samples with 2% of MgCo$_x$Ni$_{1-x}$SiO$_4$ (0.0 ≤ x ≤ 1.0) solid solutions at 1200 °C. Ni(II) CN = 6: (F) $^3A_2 \rightarrow ^3T_2$, (S) $^3A_2 \rightarrow ^3T_1$, (T) $^3A_2 \rightarrow ^3T_1$(P). Co(II) CN = 6: (1) $^4T_1 \rightarrow ^4T_2$, (2) $^4T_1 \rightarrow ^4A_2$, (3) $^4T_1 \rightarrow ^4T_1$(P). Co(II) CN = 4 (tetrahedral coordination): (4) $^4A_2 \rightarrow ^4T_1$(P).

Table 8
CIE L* a* b* colour parameters, chroma (C*) and tone (H*) from glazed tiles obtained from MgCo$_x$Ni$_{1-x}$SiO$_4$ (0.0 ≤ x ≤ 1.0) compositions fired at 1200 °C.

x	L*	a*	b*	C*	H* (°)	Colour observed
0.00	43.53	+17.54	+45.19	48.47	68.79	Beige
0.25	19.50	+2.73	+9.56	9.94	74.06	Olive green
0.50	9.44	- 0.55	- 6.08	6.10	264.83	Dark bluish green
0.75	6.37	- 0.16	- 16.21	16.21	269.43	Dark blue
1.00	3.36	+1.93	- 23.39	23.47	274.72	Dark blue

solutions fired at 1200 °C can be used in ceramic industry by decreasing the content of nickel and cobalt with respect to that existing in the Ni$_2$SiO$_4$ and Co$_2$SiO$_4$ compounds, thus producing a new, more ecological palette of ceramic colours. The observed colour (beige, green or blue) of the glazed tiles is due to the Ni(II)/Co(II) ratio as pink solid solutions dissolve in the glazes. Reproducibility will be possible if the composition is the same. A higher amount of Ni(II) and Co(II) is not necessary to develop intense green and blue colorations. Partial change of M(II) (M = Ni, Co) by Mg(II) decreases the price of raw materials too.

Declaration of competing interest

The authors declare that they have no known competing financial interests or personal relationships that could have appeared to influence the work reported in this paper.

Acknowledgements

References

[1] CPMA Classification and Chemical Descriptions of the Complex Inorganic Color Pigments. Complex Inorganic Color Pigments Committee, fourth ed., Color Pigments Manufacturers Association, Inc., 2010.

[2] C. Molinari, S. Conte, C. Zanelli, M. Ardit, G. Cruciani, M. Dondi, Ceramic pigments and dyes beyond the inkjet revolution: from technological requirements to constraints in colorant design, Ceram. Int. 46 (2020) 21839–21872.

[3] Inorganic Crystal Structure Database (ICSD Web). Fachinformationszentrum (FIZ, Karlsruhe, Germany).

[4] O. Tamada, K. Fujino, S. Sasaki, Structures and electron distributions of alpha-Ni$_2$SiO$_4$ (olivine structure), Acta Crystallogr. B39 (1983), https://doi.org/10.1107/S0108768183003250, 692-687.

[5] H.M. Rietveld, A profile refinement method for nuclear and magnetic structures, J. Appl. Crystallogr. 2 (1969) 65–71.

[6] J. Rodriguez-Carvajal (September 2018-ILL-JRC), Fullprof.2k Computer Program, Version 6.50, (France).

[7] L. Chapon, , Rutherford Appleton Laboratory, UK, J. Rodriguez-Carvajal, Institut Laue Langevin, France, FPStudio Computer Program, Version 2.0, August 2008.

[8] D. Boström, Cation ordering at 1300 °C in the (Ni,Mg)-Olivine solid solutions series, Acta Chem. Scand. 43 (1989) 116–120.

[9] M. Müller-Sommer, R. Hock, A. Kirfel, Rietveld refinement study of the cation distribution in (Co,Mg)-olivine solid solution, Physical Chemistry Mineral 24 (1997) 17–23, https://doi.org/10.1007/s002690050013.

[10] C. Michael B- Henderson, Simon A.T. Rodfern, Ronald I. Smith, Kevin S. Knight, John M. Chamack, Composition and temperature dependence of cation ordering in Ni-Mg olivine solid solutions: a time-of-flight neutron powder diffraction and EXAFS study, Am. Mineral. 86 (2001) 1170–1187.

[11] Yoshito Matsui, Yasuhito Syono, Unit cell dimensions of some synthetic olivine group solid solutions, Geochem. J. 3 (1968) 51–59.

[12] A. Zahn, P. Schreiter, Lattice constants and site preference in the system Ni$_2$SiO$_4$-Co$_2$SiO$_4$, Cryst. Res. Technol. 23 (1) (1988) 69–75, https://doi.org/10.1002/crat.2170230110.

[13] Ch-Ch Lin, Vibrational Spectroscopic study of the system α-Co$_2$SiO$_4$-α-Ni$_2$SiO$_4$, J. Solid State Chem. 157 (2001) 102–109.

[14] A. Sazonov, M. Meuen, V. Kalser, G. Heger, D. Trots, M. Merz, Structural behaviour of synthetic Co2SiO4 at low temperatures, Acta Crystallogr. B64 (2008) 661–668.

[15] M.A. Tena, Rafael Mendoza, Camino Trobajo, José R. García, Santiago García-Granda, Ceramic pigments from Co$_x$Ni$_{3-x}$P$_2$O$_8$ (0 ≤ x ≤ 3) solid solutions, Ceram. Int. 47 (21) (2021) 29888–29899, https://doi.org/10.1016/j.ceramint.2021.07.162.

[16] M.A. Tena, Rafael mendoza, Camino Trobajo, Santiago García-Granda, Cobalt minimisation in violet Co$_3$P$_2$O$_8$ pigment, Materials 15 (2022) 1111, https://doi.org/10.3390/ma15031111.

[17] Commission Internationale del'Eclairage (1978), Recommendations on Uniform Color Spaces, Color Difference Equations, Psychometrics Color Terms, Supplement No. 2 to CIE Publication No. 15 (E1-1.31), Bureau Central de la CIE, Paris, 1971.

[18] M. Pachitariu, C. Stringer, Cellpose 2.0: how to train your own model, Nat. Methods 19 (2022) 1634–1641, https://doi.org/10.1038/s41592-022-01663-4.

[19] D. Legland, I. Arganda-Carreras, P. Andrey, MorphoLibJ: integrated library and plugins for mathematical morphology with ImageJ, Bioinformatics (2016), btw413, https://doi.org/10.1093/bioinformatics/btw413.

[20] L. Torre-Fernández, C. Trobajo, I. de Pedro, B.F. Alfonso, O. Fabelo, J.A. Blanco, J.R. García, S. García-Granda, Ammonium-cobalt-nickel phosphates, NH$_4$[Co$_{1-x}$Ni$_x$PO$_4$]·H$_2$O, J. Solid State Chem. 206 (2013) 75–84.

[21] M.N. Taran, G.R. Rossman, Optical spectra of Co^{2+} in three synthetic silicate minerals, Am. Mineral. 86 (2001) 889–895.

[22] M.A. Tena, R. Mendoza, C. Trobajo, J.R. García, S. García-Granda, Co$_2$P$_2$O$_7$–Ni$_2$P$_2$O$_7$ solid solutions: structural characterization and color, J. Am. Ceram. Soc. 102 (2019) 3695–3704, https://doi.org/10.1111/jace.16158.